

University of Groningen

Development and characterizations of ultra-high molecular weight EPDM/PP based TPV nanocomposites for automotive applications

Bhattacharya, Asit Baran; Raju, Aswathy T.; Chatterjee, Tuhin; Naskar, Kinsuk

Published in:
 Polymer Composites

DOI:
[10.1002/pc.25765](https://doi.org/10.1002/pc.25765)

IMPORTANT NOTE: You are advised to consult the publisher's version (publisher's PDF) if you wish to cite from it. Please check the document version below.

Document Version
 Publisher's PDF, also known as Version of record

Publication date:
 2020

[Link to publication in University of Groningen/UMCG research database](#)

Citation for published version (APA):

Bhattacharya, A. B., Raju, A. T., Chatterjee, T., & Naskar, K. (2020). Development and characterizations of ultra-high molecular weight EPDM/PP based TPV nanocomposites for automotive applications. *Polymer Composites*, 41(12), 4950-4962. <https://doi.org/10.1002/pc.25765>

Copyright

Other than for strictly personal use, it is not permitted to download or to forward/distribute the text or part of it without the consent of the author(s) and/or copyright holder(s), unless the work is under an open content license (like Creative Commons).


The publication may also be distributed here under the terms of Article 25fa of the Dutch Copyright Act, indicated by the "Taverne" license. More information can be found on the University of Groningen website: <https://www.rug.nl/library/open-access/self-archiving-pure/taverne-amendment>.

Take-down policy

If you believe that this document breaches copyright please contact us providing details, and we will remove access to the work immediately and investigate your claim.

Downloaded from the University of Groningen/UMCG research database (Pure): <http://www.rug.nl/research/portal>. For technical reasons the number of authors shown on this cover page is limited to 10 maximum.

Development and characterizations of ultra-high molecular weight EPDM/PP based TPV nanocomposites for automotive applications

Asit Baran Bhattacharya¹ | Aswathy T. Raju¹ | Tuhin Chatterjee² | Kinsuk Naskar¹ 

¹Rubber Technology Centre, Indian Institute of Technology Kharagpur, Kharagpur, West Bengal, India

²Department of Chemical Engineering, University of Groningen, Groningen, The Netherlands

Correspondence

Kinsuk Naskar, Rubber Technology Centre, Indian Institute of Technology Kharagpur, Kharagpur, West Bengal, India
Email: knaskar@rtc.iitkgp.ac.in

Abstract

This research article reports, the preparation of thermoplastic vulcanizates (TPVs) and TPV nanocomposites (TPVNs) based on EPDM and polypropylene (PP). New generation ultra-high molecular weight EPDM (UHMW-EPDM) and PP with nano-fillers (nano-clay and nano-silica) and has been studied and characterized extensively typically for automotive applications. This special type of UHM-EPDM-based TPVs exhibit superior physico-mechanical properties over conventional EPDM-based TPVs and in the presence of nano-fillers, they show even better physical properties. The TPVNs were prepared with a fixed EPDM:PP ratio and the nano fillers were varied at different concentrations. The influence of nano-fillers, especially hectorite nano-clay and nano-silica has been first explored through physico-mechanical properties. Tensile strength, elongation at break, and modulus at various strain are improved for nano-filler filled TPVNs. We have observed that due to the incorporation of nano-fillers into the TPV matrix, swelling has been decreased. From morphology (AFM, SEM) study, it is observed that the fillers are well dispersed in the TPV matrix and nano-silica fillers are well dispersed than nano-clay (hectorite). Furthermore, small-angle X-ray scattering (SAXS) studies have also been pursued to get a better insight into the TPV system. These newly developed TPVs can be used as potential candidates for application in the automotive sector.

KEYWORDS

AFM, EPDM, FESEM, nano-clay, nano-silica, PP, SAXS, thermoplastic vulcanizates

1 | INTRODUCTION

Polymer blend may be defined as a combination of two or more structurally different polymers or copolymers giving rise to materials with a range of properties, not delivered by any of the constituents. Blending of polymers is a common technique and frequently applied in order to develop a product with improved mechanical properties using inexpensive polymers. The aim of

polymer blending is to obtain materials, which as far as possible to combine the advantages, but not their disadvantages. In the last few decades, the attention has been shifted toward the development of different polymer blends, rubber blends, and polymer composites. Because, polymer or rubber blending is a technique by which a new class of materials are obtained with a wide range of different properties. Sometimes those properties are also showing synergistic effect and that is our point of

attraction. A wide range of polymer (rubber-plastic) blends are available in the market, but few of them are commercially attractive depending upon application areas. Generally, rubber-plastic blends are categorized into two categories: (a) thermoplastic elastomer (TPE) and (b) thermoplastic vulcanizates (TPVs). TPVs are prepared by dynamic vulcanization process, where rubber matrix is cross-linked while mixed with thermoplastic to make a homogeneous melt.^[1] As a result, products are obtained which consist of crosslinked rubber particles dispersed in a continuous thermoplastic matrix, that explains both elasticity and melt processability.^[2] The control in morphology is very important for this type of blends (TPVs).^[3–8] Scheme.1 demonstrates the morphology development during the process of dynamic vulcanization of TPVs.^[9] The development of morphology of TPV is liable upon different parameters, such as blend ratio of rubber and thermoplastic, viscosity ratio, shear force, and interfacial interaction between two phases. Generally, viscosity ratio between two phases plays major role on morphology development of TPV (less viscous phase is encapsulated the higher viscous phase), with the addition of curative. When curatives are added degree of crosslinking increased as well as viscosity, and also particle size decreases. The morphology development of TPV from co-continuous phase to dispersed phase is shown in Scheme 1.^[10]

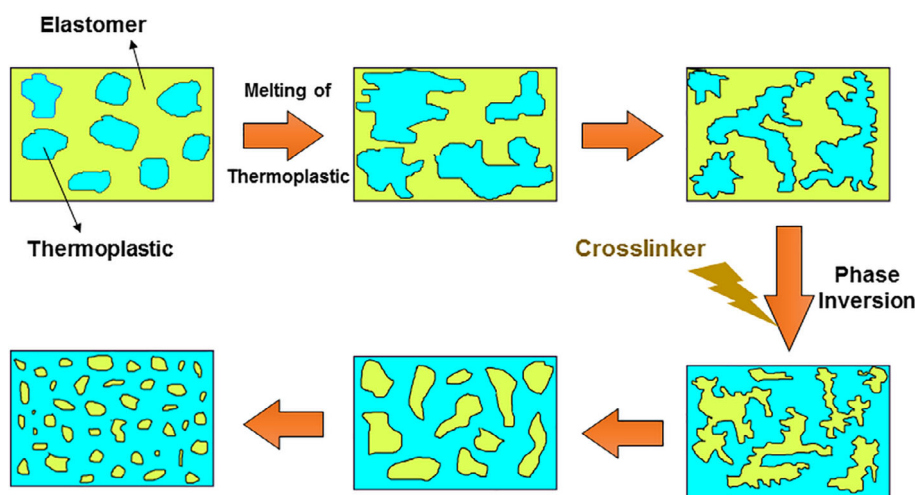
The concept of TPV was first proposed by Gessler and Haslett in 1962.^[11] TPVs are prepared by the melt mixing of thermoplastic phase (eg, PP) and elastomeric phase (eg, EPDM) and later the elastomeric phase is cross-linked and dispersed in thermoplastic phase like rubber particles.^[2,5,7] The final blend morphology of the TPV always consists of cross-linked, micron sized elastomer particles dispersed in a polymer matrix.^[11]

Since TPV is an important material for automotive applications, many attempts have been followed to

develop with different blend compositions. Abdou-Sabet and Patel has reported that morphology development during process of dynamic vulcanization for resin cured PP/EPDM TPVs.^[12] Naskar et al has reported the effect of different types of peroxides and different dosages on PP/EPDM TPVs and also discussed with the different blend ratio of PP/EPDM.^[13] Van Duin et al have reported the resin curing chemistry of TPVs and the effect of resin curing on the extrusion process of TPVs.^[14] Maiti et al studied the details of mechanical properties on gas phase EPDM/PP TPVs with various crosslinking systems. Optimized systems were compared for heat aging, recyclability, crosslink density, morphology studies, and dynamic mechanical analysis.^[15] A comprehensive overview is given by Babu et al in a review in 2010, of the recent developments of TPVs. Therefore, they lend themselves to a broad range of applications in various fields.^[5]

Dicumyl peroxide (DCP) cured TPVs based on blends of m-EPM and polypropylene (PP) using maleated-PP as a compatibilizer have been reported, by Chatterjee et al. in 2008. Significant improvement in tensile strength (TS), modulus, and impact strength of TPVs have been achieved. Morphology study shows that nano-silica is uniformly dispersed in the polymer matrices.^[16] Soares et al. in 2019 have reported TPVs based on PP and carboxylated nitrile rubber (XNBR) with improved mechanical properties were prepared by dynamic vulcanization using DCP in combination with N,N'-mphenylene-bis-maleimide (BMI) as a cross-linking system.^[11]

In the past few decades, there is a good demand in research on polymer-clay nanocomposites, because it can offer enhanced fire, mechanical, and barrier properties compared to polymer composites containing traditional fillers. Work has been conducted on a wide variety of polymers, including thermoplastics, such as styrenics, and polyolefins. There are several types of nano-clays used for research purpose, such as layered double



SCHEME 1 Development of morphology during dynamic vulcanization [Color figure can be viewed at wileyonlinelibrary.com]

hydroxide (LDH), montmorillonite (MMT), bentonite (aluminum phyllosilicate clay), and hectorite.^[17] When organically-modified layered-silicate clays are used, in general, good dispersion of the clay in the polymer can be achieved. Where mechanical properties have been examined, they appear to be improved by the addition of a small amount of clay, but are decreased with larger amount of clays.^[17–20]

The silica nano fillers (especially SiO₂ nano particles) have higher aspect ratio than typical microscopic aggregates and it is attractive for polymer reinforcement. Polymer-clay nanocomposites had shown drastic enhancement in mechanical properties (modulus and TS), thermal properties (heat resistance and flammability), and barrier properties. But, the greatest challenge in polymer nano technology is to uniformly disperse these nano dimensioned fillers, which offer numerous advantages over conventional micrometer-sized fillers. The interest in the area of polymer nanocomposites is many folds. First, the present understanding of composite behavior does not fully satisfy or predict from a scientific standpoint why these systems are superior in many of its properties.^[21,22]

Therefore, the primary objective of this work is to develop TPV nano composite (TPVNs) by using new generation UHMW EPDM rubber with nano-clay and nano-silica for the application in automotive sector and it should also exhibit very good physico-mechanical properties. To prepare a new generation TPVNs, EPDM rubber, and PP thermoplastic have been taken for this study. EPDM has very good weather resistance and heat resistance property, which is very important for automotive applications. PP has good TS and very good compatible with EPDM rubber. Further the solubility parameter of EPDM and PP are 17.2 and 16.6 J^{1/2} cm^{-3/2}, respectively, this also indicates the possibility of higher degree of compatibility between these two polymers.^[23] Finally, in the present work, we have investigated the physico-mechanical behavior of the blends (EPDM/PP) with different nanofillers ratios and also the morphological analysis

with special reference to atomic force microscope (AFM), and field emission electron microscope (FESEM).

In this current study, we used the latest developed UHMW EPDM rubber, specially designed for exposure to high temperature to prepare new generation TPVs. This grade having comparable Mooney viscosity with natural rubber as high ML(1 + 4)_{@125°C} and a tailored molecular structure enabling it to match the strength and resilience of NR. Not only the EPDM but also, we have used a different type of random copolymer PP not used commonly, which was also highly recommended for automotive applications.

2 | EXPERIMENTAL

2.1 | Materials

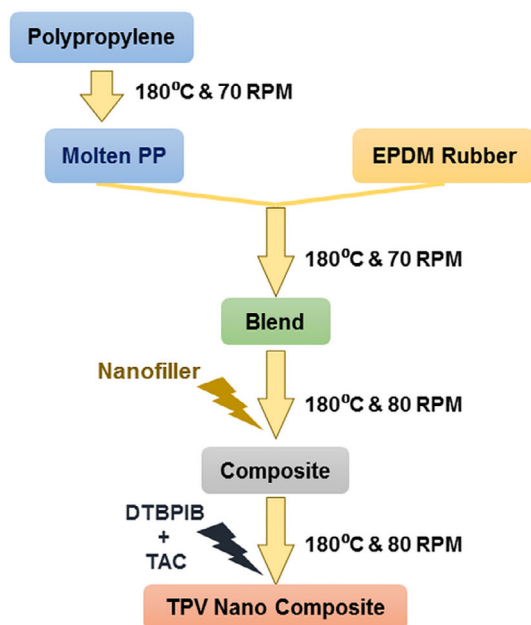
A newly developed UHMW grade of EPDM was used. It has a uniformly distributed co-monomer with 62% ethylene content. It is designed to improve the dynamic properties. PP (SR20NC) in the granular form was used which is random copolymer with a density of 0.92 g/cc. The details of the polymers are tabulated in the Table 1. Perkadox 14-40B, [Di-(2- tert butyl peroxy isopropyl) benzene] (DTBPIB) was used as a crosslinker of the EPDM rubber phase, procured from Akzo Nobel, The Netherlands, with 40% concentrated, dispersed in Calcium carbonate carrier materials. Triallyl cyanurate (TAC) was used with peroxide to prevent the side reaction of the PP for the presence of peroxide. Hectorite nano-clay, layered mineral silicates was procured from BYK additives and nano-silica (particle size ~10 nm) was procured from Sigma Aldrich.^[24]

2.2 | Preparation of the blends

To prepare the TPV and TPVNs, UHM-EPDM and PP (constant ratio 100:50) was, mixed in a Haake PolyLab

TABLE 1 Characteristics of polymers

Parameters	Polypropylene (PP)	EPDM rubber
Source	Reliance Industries Limited, India	ARLANXEO, The Netherlands
Grade	SR20NC	Keltan 9565Q
ENB content (%)	—	5.5
Ethylene content (%)	—	62
Melt flow index (230°C/2.16 kg)	1.9 g / 10 minutes	—
Density (gm cc ⁻¹)	0.86	0.92
Oil content (%)	—	50
Mooney viscosity (ML _(1 + 4) @125°C)	—	85 ± 2



SCHEME 2 Preparation of thermoplastic vulcanizates (TPVs) [Color figure can be viewed at wileyonlinelibrary.com]

Rheomix (Germany) internal mixers, having a mixing chamber volume of 85 cm³ at 180°C to 190°C for 7 to 7.5 minutes. First PP was added and it was allowed to melt for 2 minutes at 70 rpm. Then EPDM was added and the mixing was continued to 4 minutes. Nano fillers were then added after EPDM and the mixing was continued to 6 minutes. Finally, curative (peroxide and co-agents) were added slowly and mixing was continued up to 7 to 7.5 minutes. The scheme of preparation of the TPV nanocomposites is depicted in Scheme 2.

The mixes so obtained were sheeted under hot conditions in an open mill set at 2 mm nip gap. The sheets were compression molded between Teflon sheets for 4 minutes at 190°C at a pressure of 5 MPa in an electrically heated hydraulic press (Moore Hydraulic Press, England). The molded sheets were cooled under pressure to maintain the overall dimensional stability of the molded articles. Table 2 shows various blends prepared for this study.

2.3 | Testing and characterizations

2.3.1 | Mechanical properties

The mechanical properties of the blends were determined as per ASTM D 412. A dumbbell specimen was placed in the grips of the testing machine, using care to adjust the specimen symmetrically to distribute tension uniformly over the cross-section. A Hounsfield H25KS universal testing machine at a crosshead speed of 200 mm min⁻¹

was used for the TPV samples.^[25] The hysteresis measurement of the blends has been done in a Zwick RoelZ010 UTM, the tensile testing specimen was used. The loading and unloading speed was 200 mm min⁻¹. The hysteresis measurement was carried out in constant strain amplitude mode. All sample testing was carried out at ambient temperature.

2.3.2 | Crosslink network characterization

To measure the crosslink density of the EPDM in presence of PP ($\nu_{EPDM + PP}$), equilibrium solvent swelling method was carried out on the PP/EPDM TPV samples. The crosslink density was calculated using modified Flory-Rehner equation^[26] as shown below (Equation (1)). In case of TPVs, crosslinked EPDM is surrounded in the relatively less swellable matrix like PP. A circular piece of 2 mm thickness was made to swell in cyclohexane for 48 hours to achieve equilibrium swelling condition. Initial weight, swollen weight, and de-swollen or dried weight were measured and substituted in the following Equation (1)

$$\nu_{EPDM + PP} = -\frac{1}{V_s} \times \frac{\ln(1 - V_r) + V_r + \chi(V_r)^2}{V_r^{\frac{1}{3}} - 0.5V_r}, \quad (1)$$

where ν is the number of moles of effectively elastic chains per unit volume of EPDM rubber (mol mL⁻¹) (crosslink density), ($\nu_{EPDM + PP}$) crosslink density of EPDM phase in the presence of PP (overall crosslink density), V_s is the molar volume of cyclohexane (cm³ mol⁻¹), χ is the polymer swelling agent interaction parameter, and the value is 0.306 and V_r is the volume fraction of EPDM in the swollen network, which can be expressed by

$$V_r = \frac{1}{A_r + 1} \quad (2)$$

where A_r is the ratio of the volume of absorbed cyclohexane to that of EPDM after swelling.^[27]

2.3.3 | Scanning electron microscopy (SEM)

The morphology of the TPV samples was observed through a Field Emission Scanning Electron Microscope, Merlin (Germany). All the samples were first cryo-fractured in liquid nitrogen then etched out the PP phase in hot Xylene at 100°C for 1 hour and finally the samples

TABLE 2 Designation of the nano TPVs made from PP/EPDM (in phr)

Sample name	Rubber hydrocarbon	PP	Nano clay	Nano silica	DTBPIB	TAC
E ₁₀₀ P ₅₀	100	50	0	0	3	2
E ₁₀₀ P ₅₀ H ₁	100	50	1	0	3	2
E ₁₀₀ P ₅₀ H ₃	100	50	3	0	3	2
E ₁₀₀ P ₅₀ H ₅	100	50	5	0	3	2
E ₁₀₀ P ₅₀ H ₇	100	50	7	0	3	2
E ₁₀₀ P ₅₀ S ₁	100	50	0	1	3	2
E ₁₀₀ P ₅₀ S ₃	100	50	0	3	3	2
E ₁₀₀ P ₅₀ S ₅	100	50	0	5	3	2
E ₁₀₀ P ₅₀ S ₇	100	50	0	7	3	2

Abbreviations: PP, polypropylene; TAC, triallyl cyanurate; TPVs, thermoplastic vulcanizates. The bold values signifies the amount of the nano-fillers.

were dried in hot air oven at 70°C for 6 hours. All the sample surfaces were sputtered with gold to provide enhanced conductivity.^[27]

2.3.4 | Atomic force microscopy

Tapping mode atomic force microscopy, AC-AFM (Agilent 5500 Scanning Probe Microscope) was used to investigate the morphology of the TPV samples. The cantilever frequency was 150 kHz, and the force constant was 42 N m⁻¹.^[10]

2.3.5 | SAXS study

To study the scattering behavior of the nano fillers in the TPV nanocomposites, small-angle X-ray scattering (SAXS) was studied in Anton Paar SAXSpace with CuK α ($\alpha = 0.1542$ nm) X-Rays. In SAXS mode, the sample was positioned far away from the detector and the data recorded.

3 | RESULTS AND DISCUSSION

3.1 | Mixing energy curve

The effect of the dynamic vulcanization of EPDM/PP pristine blend (E₁₀₀P₅₀) and EPDM/PP blends by different nano-fillers were seen in the torque-time graph during mixing in the Haake internal mixer (Figure 1). In Figure 1, four distinct stages of mixing have been observed. Stage A indicates the melting of the PP at 30 rpm for 2 minutes, followed by adding of EPDM rubber melt mixing at 50 rpm at stage B up to 4.5 minutes. At stage C, nano-fillers are added for TPVNs and mixed at

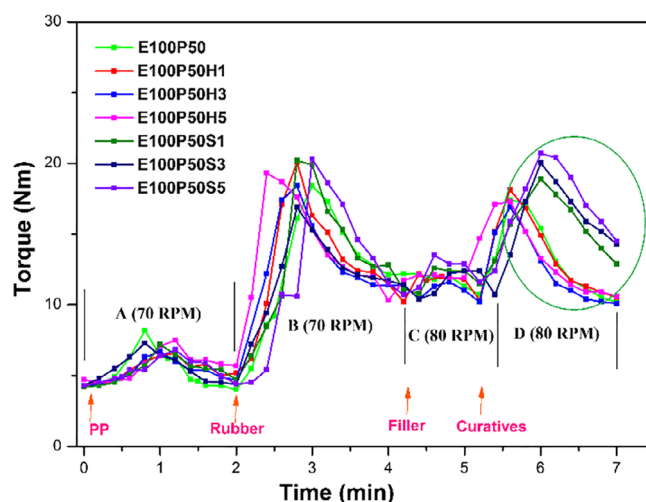


FIGURE 1 Mixing energy curve [Color figure can be viewed at wileyonlinelibrary.com]

80 rpm up to 5 minutes and finally curing agent (peroxide + coagent) added at 80 rpm and dumped at 7 minutes. For all the batches, dynamic vulcanization time was 2 minutes. From Figure 1, it is clearly visible that the effect of dynamic vulcanization and the torque has been rising sharply due to crosslinking of EPDM phase at stage D. The effect of addition of nano filler has also been clearly visible at stage D. Due to the addition of nano-clay, there is not much change in torque at stage D with respect to pristine blend (E₁₀₀P₅₀), but there is rise in the torque of the nano-silica filler added blends due to the more reinforcement in the PP/EPDM matrix by nano-silica.

3.2 | Physico-mechanical properties

The stress-strain behavior properties of the PP/EPDM TPVNs are shown in Figure 2 and tabulated in Table 3. The effect of dynamic vulcanization is clearly visible from

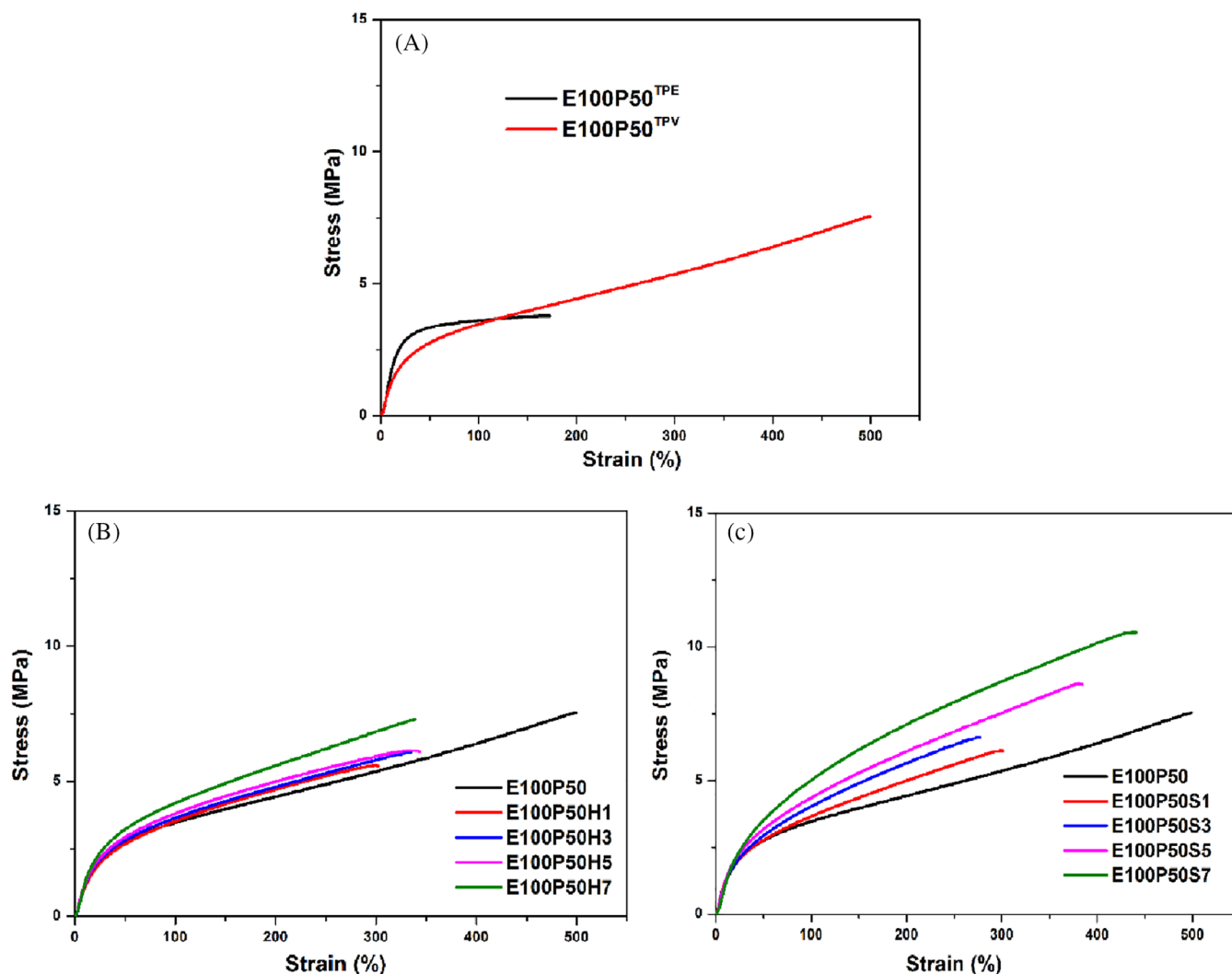


FIGURE 2 Stress-strain behavior of the blends: A, EPDM/PP thermoplastic elastomer (TPE) and thermoplastic vulcanizate (TPV); B, nano-clay filled TPVs with pristine TPV ($E_{100}P_{50}$); and C, nano-silica filled TPVs with pristine TPV ($E_{100}P_{50}$) [Color figure can be viewed at wileyonlinelibrary.com]

Figure 2A, PP/EPDM thermoplastic elastomer uncrosslinked blend shows the TS below 5 MPa and elongation at break (%EB) below 200% but the PP/EPDM TPV shows TS 7.5 MPa and EB 490%. As the EPDM rubber phase has crosslink due to the presence of the peroxide and coagent, the mechanical properties also improved.

Stress-strain behavior of the TPVNs is shown in Figure 2B (nano-clay) and Figure 2C (nano-silica). The modulus of the sample is mentioned in Table 3 at different elongation (100%, 200%, and 300%). It clearly shows that the effect of the two different type of nano-fillers in the TPV matrix. The TS and modulus for the nano-clay TPVs is initially decreasing, as we are incorporating the nano-fillers than the pristine blend but as the nano-filler concentration increases the TS and modulus also increasing due to the reinforcement behavior of the nano-fillers. But the EB% has decreased due to decrease of the mobility of the rubber

chain in the TPV matrix. For the nano-silica TPVNs, the TS and the modulus is higher than the nano-clay TPVNs. Such variation in the mechanical properties has been seen because of the structure of the nano-fillers, that is, nano-silica is particulate type structure that is why incorporation in the TPV matrix is very easier than the nano-clay. As the nano-clay structure is a layered silicate structure, so it is difficult to disperse layered filler in the TPV matrix. Hence, we can see that at 7 phr nano-filler loading the TS and modulus is higher than the pristine blend only the EB% is less but it is also the more than 250%.

3.3 | Overall crosslink density

Crosslinked density ($\nu_{EPDM + PP}$) study has been done to characterize the crosslinked network of the EPDM rubber

TABLE 3 Mechanical properties of the various blends

Samples	Tensile strength (MPa)	Changes with respect to $E_{100}P_{50}$ (%)	Elongation at break (%)	Changes with respect to $E_{100}P_{50}$ (%)	Modulus (MPa)			Modulus changes with respect to $E_{100}P_{50}$ (%)		
					100%	200%	300%	100%	200%	300%
$E_{100}P_{50}$	7.5	—	497	—	3.5	4.4	5.4	—	—	—
$E_{100}P_{50}H_1$	5.6	-26	308	-38	3.5	4.7	5.6	+01	+06	+04
$E_{100}P_{50}H_3$	6.1	-19	333	-33	3.6	4.8	5.8	+05	+09	+08
$E_{100}P_{50}H_5$	6.1	-18	331	-33	3.8	5.0	5.9	+10	+13	+10
$E_{100}P_{50}H_7$	7.3	-03	334	-33	4.2	5.6	6.8	+21	+27	+28
$E_{100}P_{50}S_1$	6.1	-18	302	-39	3.7	5.0	6.1	+05	+13	+14
$E_{100}P_{50}S_3$	6.6	-12	274	-45	4.0	5.7	—	+16	+29	—
$E_{100}P_{50}S_5$	8.6	+15	379	-24	4.4	6.1	7.5	+25	+38	+40
$E_{100}P_{50}S_7$	9.9	+32	387	-22	5.0	7.1	8.7	+44	+60	+63

phase in the TPV has been measured and shown in the Figure 3. At a constant amount of the peroxide and coagent the value of overall crosslink density has decreased with respect to the pristine TPV because of the addition of the nano-filler the crosslinking of the rubber phase is disturbed. For nano-clay TPVNs, the value of the overall crosslink density is less than the nano-silica TPVNs. This proves that the nano-silica filler is giving more reinforcement than nano-clay fillers.

3.4 | Hysteresis study of the blends

The hysteresis study provides the information of the structural changes of polymeric materials under strain and cyclic deformation. The TPV and TPVN samples were subjected to uniaxial tensile deformation at a constant speed of 200 mm min^{-1} up to 100% strain. As we know that polymeric materials pose viscoelastic nature, the energy applied may not balance with the energy released, and the stretching and recoiling curves (loading and unloading curves) form a loop called hysteresis loop.^[5] In Figure 4, the hysteresis loop of cyclic tensile curves of pristine TPV ($E_{100}P_{50}$), nano-clay TPVN ($E_{100}P_{50}H_1$), and nano-silica TPVN ($E_{100}P_{50}S_1$) at a constant strain of 100% are shown. A linear elastic nature followed by yielding (Boyce et al)^[28] has seen during stretching of the blends, which is a characteristic feature of the thermoplastic materials.

The TPVs and TPVNs are showing strain hardening after yielding. Soliman et al) reports that the deformation mechanism of PP/EPDM TPVs is that the yielding and buckling is happened by PP and recovering tendency by the crosslinked rubber particles (Figure 4B). When it is stretched, the PP is acting as glue between the

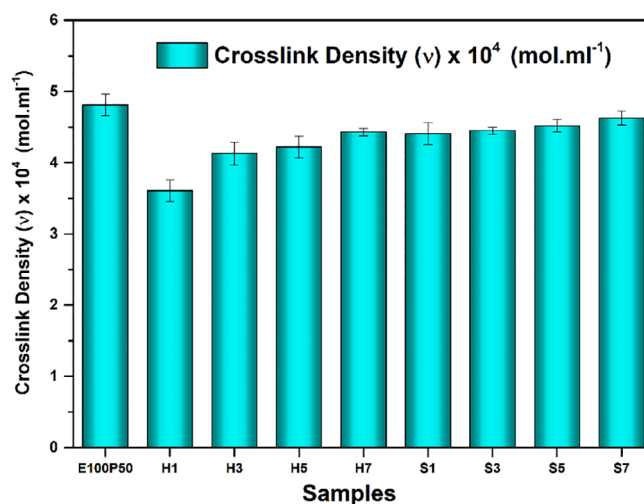


FIGURE 3 Crosslink density of various thermoplastic vulcanizates (TPVs) [Color figure can be viewed at wileyonlinelibrary.com]

crosslinked rubber particles and the yielding direction goes perpendicular to the load. Again, when it is trying to recover, the yielded PP fraction is partially pulled back by the recovering force of the crosslinked rubber particles.

In Table 4 and Figure 4A we can see that, after the first cycle significant softening is occurring followed by gradual softening happens with the increase in number of cycles from one to three. The reason behind this phenomenon may be due to disentanglement and slippage of polymer chains. The dynamically vulcanized blend both pristine TPV and TPVNs decrease the setting behavior and lowers the energy loss, which is a characteristic feature of an elastomeric material. In Table 4, we have shown the hysteresis results for all the blends but for better understanding, we have plotted only pristine TPV

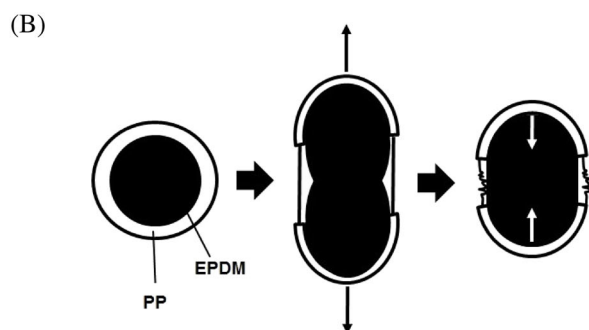
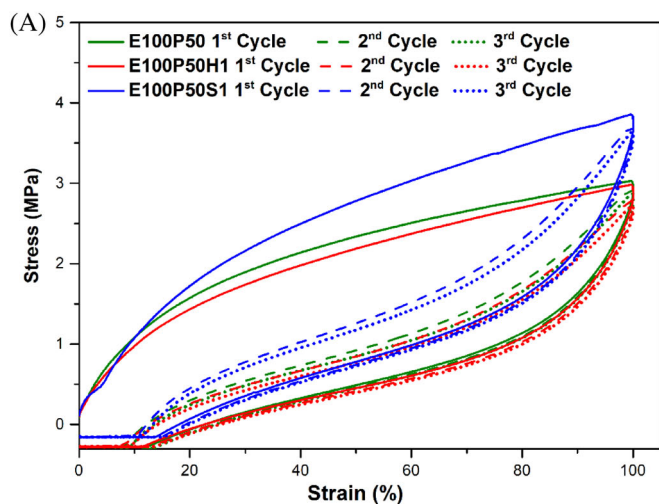


FIGURE 4 A, Hysteresis loops of the thermoplastic vulcanizate (TPV) and TPV nanocomposites (TPVNs) during cyclic tension at 100% strain, and B, deformation mechanism model of TPVs suggested by Soliman et al.^[34] [Color figure can be viewed at wileyonlinelibrary.com]

(E₁₀₀P₅₀), nano-clay TPVN (E₁₀₀P₅₀H₁), and nano-silica TPVN (E₁₀₀P₅₀S₁). Furthermore, when we are comparing the hysteresis behavior between the pristine TPV and TPVNs, it is seen that TPVNs are showing less setting behavior than pristine one, especially nano-silica TPV. The reason may be the better physical entanglement in the matrix and better dispersion of the nano-silica.

3.5 | Reprocessability study of the blends

The physico-mechanical properties of the TPV and TPVNs after two cycles of the remixing and remolding are shown in Table 5. The changes in the mechanical properties all are in the acceptable limit. For the nano-silica TPVs after remixing, the mechanical properties has been increased little bit may be due to better dispersion of the nano-silica. But all the results are indicating satisfactory level of reprocessability of the blends and ideal behavior as thermoplastic elastomers, which is essential for reprocessing.

3.6 | SAXS study of TPV and TPVNs

The operation of a scattering instrument is identical to the process interaction between matter and incoming radiation that takes place in a microscope, its result is complementary to that of a microscope. Scattering can occur with or without loss of energy. This means that the scattered radiation can have a different wavelength than the incident radiation (Compton scattering) or it can have the same wavelength (Rayleigh or Thomson scattering). Compton scattering is produced when a photon hits an electron and is bounced away. The photon loses a fraction of its energy, which is taken over by the electron. The scattered radiation has a different wavelength and has no particular phase relationship (incoherent scattering) with the incident radiation. It cannot produce interference phenomena and therefore does not carry structure information.^[29] To investigate the nanocomposite materials, especially when the nano-fillers are surrounded in a matrix, scattering phenomenon is a very important tool. To know the nature of the dispersion of the nano particles in a polymer matrix (EPDM/PP), the basic theory of scattering, such as nanoparticles and dispersed medium have uniformity and there is no presence of special orientation with respect to the incident beam direction. For better understanding of the aggregation of the nanoparticles,

TABLE 4 Results of hysteresis test at constant strain of 100%

Samples	Max. stress (MPa)			Stress decay (%) at w.r.t. first cycle	
	First Cycle	Second cycle	Third cycle	Second cycle	Third cycle
E ₁₀₀ P ₅₀	2.9	2.8	2.8	-3.4	-3.4
E ₁₀₀ P ₅₀ H ₁	2.8	2.7	2.6	-3.6	-7.1
E ₁₀₀ P ₅₀ H ₃	3.0	2.9	2.9	-3.3	-3.3
E ₁₀₀ P ₅₀ H ₅	2.7	2.6	2.6	-3.7	-3.7
E ₁₀₀ P ₅₀ S ₁	3.7	3.6	3.5	-2.7	-5.4
E ₁₀₀ P ₅₀ S ₃	3.6	3.5	3.5	-2.8	-2.8
E ₁₀₀ P ₅₀ S ₅	3.4	3.3	3.2	-2.9	-5.9

TABLE 5 Results of the reprocessability study of the various blends

Samples	Tensile strength (MPa)			100% Modulus (MPa)		
	First cycle	Second cycle	Third cycle	First cycle	Second cycle	Third cycle
E ₁₀₀ P ₅₀	7.5	6.3	5.9	3.5	3.1	2.9
E ₁₀₀ P ₅₀ H ₁	5.6	5.8	5.4	3.5	3.0	2.8
E ₁₀₀ P ₅₀ H ₃	6.1	5.4	5.0	3.6	3.0	2.8
E ₁₀₀ P ₅₀ H ₅	6.1	5.1	4.9	3.8	3.0	2.7
E ₁₀₀ P ₅₀ S ₁	6.1	6.7	7.1	3.7	3.1	2.9
E ₁₀₀ P ₅₀ S ₃	6.6	7.4	7.8	4.0	3.3	3.0
E ₁₀₀ P ₅₀ S ₅	8.6	8.2	7.9	4.4	3.3	3.0

colloidal physics can be followed.^[30] To study the structural changes of the TPVs in the presence of the nano-fillers, SAXS study has been done. In Figure 5, the SAXS pattern of the TPV and TPVNs are shown. The SAXS experiment setup is very simple: a thin film of the TPV sample usually placed in front of monochromatic X-ray beam; the intensity of the scattered X-ray is detected by an X-ray detector. The SAXS pattern obtained from the instrument with the sample to detector distance of 317 mm and the scattering (q) range of 0.10 to 7.00 \AA^{-1} , ($q = 4\pi/\lambda \cdot \sin(\theta/2)$), where $\lambda = 1.545 \text{\AA}$ is the X-ray wavelength and q is the scattering angle.

Scattering intensity (I) vs scattering vector (q) has plotted in Figure 5. So, as the scattering intensity will increase the dispersion of the fillers in the samples. In the Figure, it is clearly seen that as the amount of the nano-clay increased the scattering intensity has decreased, but for the nano-silica as the amount increased scattering intensity increased and the pristine TPV is showing the least scattering intensity among all the blends. So, we can conclude that the nano-silica fillers are more dispersed than the nano-clay filler and the effect of dispersion has reflected to the mechanical properties.

3.7 | Morphology study

3.7.1 | Field emission scanning electron microscope

The mechanical properties of the TPVs depend not only on the blend ratio but also on the morphology of the blends. According to Chung et al the factors affecting to the morphology of the TPVs are blend ratio, interfacial tension and viscosity ratio and so on.

The FESEM study provides that there is a change in morphology after dynamic vulcanization.

Due to the, higher viscosity and propylene units present in EPDM (partially miscible with the PP-matrix

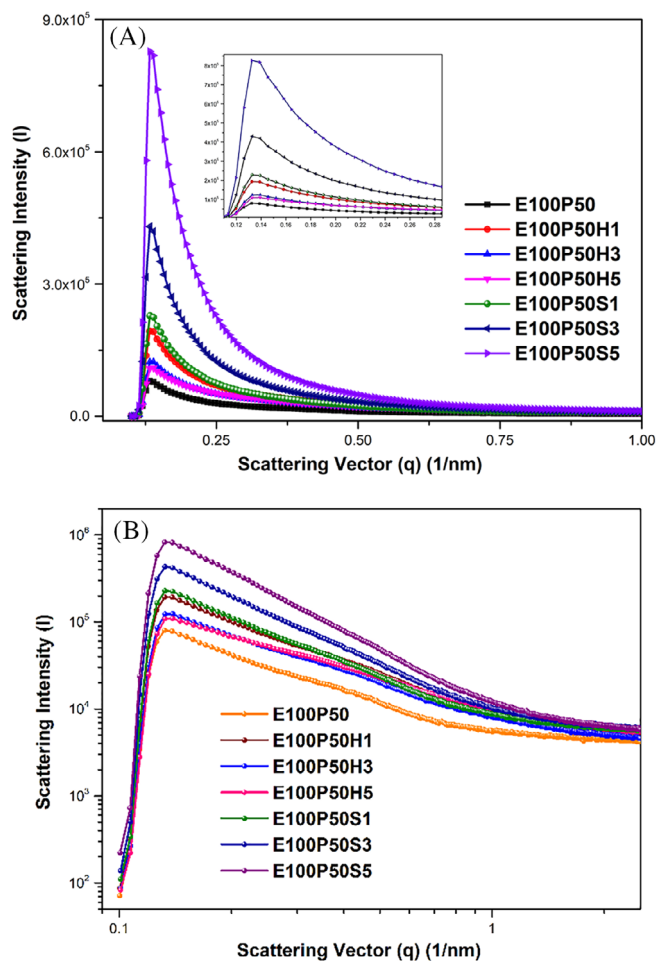


FIGURE 5 SAXS pattern of the thermoplastic vulcanizate (TPV) and TPV nanocomposites (TPVNs), scattering intensity [I] vs scattering vector [q] [Color figure can be viewed at wileyonlinelibrary.com]

phase in the molten stage), leads to the formation of deformed and irregular shaped particles. Similar morphology was observed by Babu et al while comparing uncrosslinked PP/EOC with PP/EPDM blends.^[31]

In the Figure 6A, PP/EPDM uncrosslinked blend is shown and we can see the co-continuous morphology. In

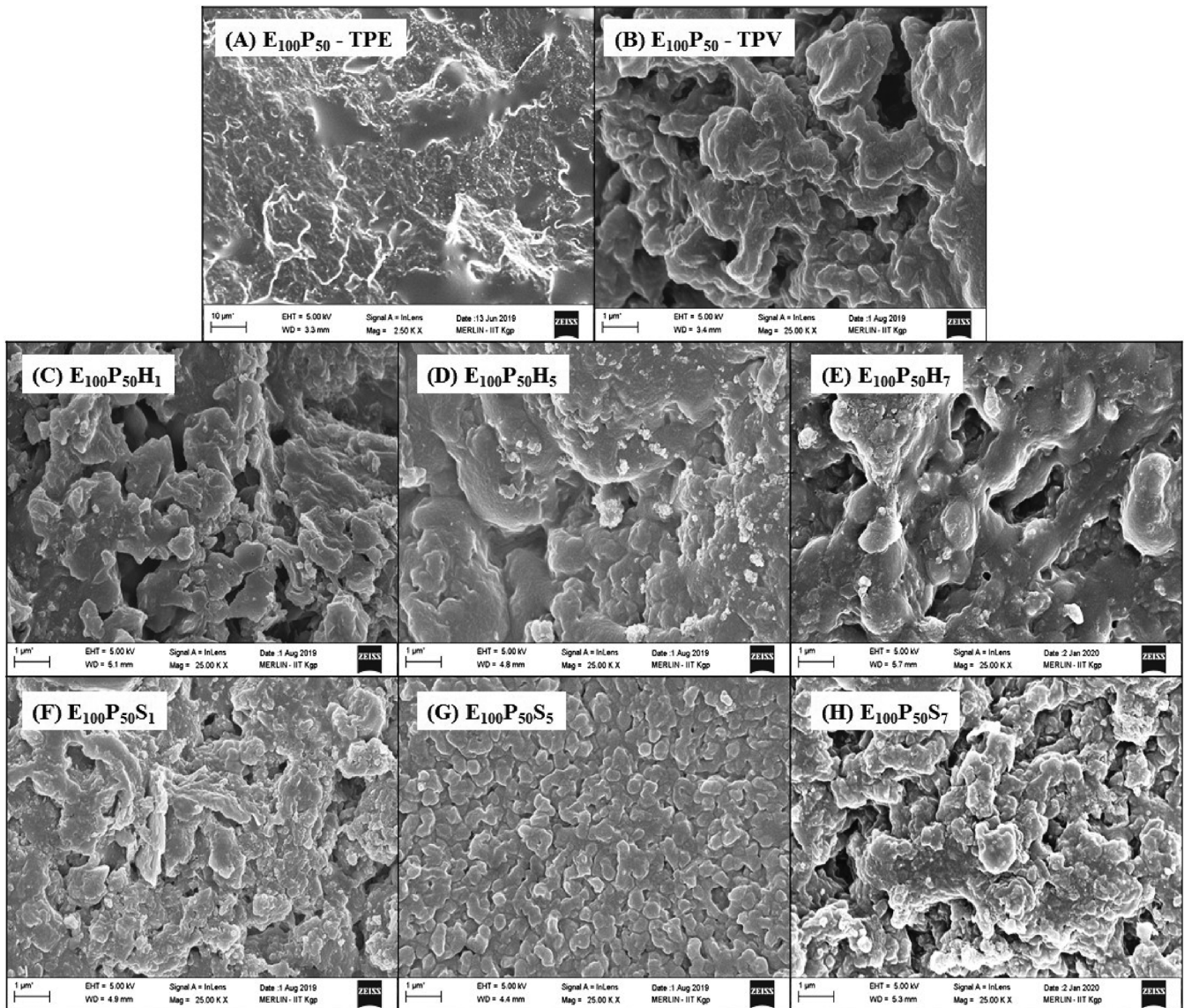


FIGURE 6 FESEM images of A, $E_{100}P_{50}$ -TPE; B, $E_{100}P_{50}$ -thermoplastic vulcanizate (TPV); C, $E_{100}P_{50}H_1$; D, $E_{100}P_{50}H_5$; E, $E_{100}P_{50}H_7$; F, $E_{100}P_{50}S_1$; G, $E_{100}P_{50}S_5$; and H, $E_{100}P_{50}S_7$

Figure 6B-H we can see the dynamically vulcanized blends of $E_{100}P_{50}$, $E_{100}P_{50}H_1$, $E_{100}P_{50}H_5$, $E_{100}P_{50}H_7$, $E_{100}P_{50}S_1$, $E_{100}P_{50}S_5$, and $E_{100}P_{50}S_7$, respectively. EPDM prefers to exist in a dispersed phase because of the higher viscosity ratio in PP/EPDM. However, by dynamic vulcanization, a complete phase transition (inversion) occurs, that is, co-continuous morphology is changed into dispersed phase morphology. The less viscous PP encapsulates the more viscous crosslinked rubber particles to minimize the mixing energy.^[5,32]

In Figure 6D, the PP phase less etched out for $E_{100}P_{50}H_5$ due to the better interaction between PP and nano-clay. There is not much change in pristine sample ($E_{100}P_{50}$) and $E_{100}P_{50}H_1$ as only 1 phr nano-clay has been added, whereas for $E_{100}P_{50}S_1$, the morphology is elongated and lamellar type morphology

has been observed. On increasing of the nano-silica in case of $E_{100}P_{50}S_3$, prominent and equiposed domain size morphology has achieved but for $E_{100}P_{50}S_7$ due to increasing of the nano-silica inhomogeneity arises. For $E_{100}P_{50}H_7$ nano-clay filler, percolation limit for holding the phase has crossed and PP domain has etched out and living behind the holds and pits. Therefore, from the FESEM study we can say that, domain size formation capability is nano-silica than the nano-clay.

3.7.2 | AFM study

The AFM can provide an insight of surface topography and surface heterogeneity of polymer systems. AFM, phase

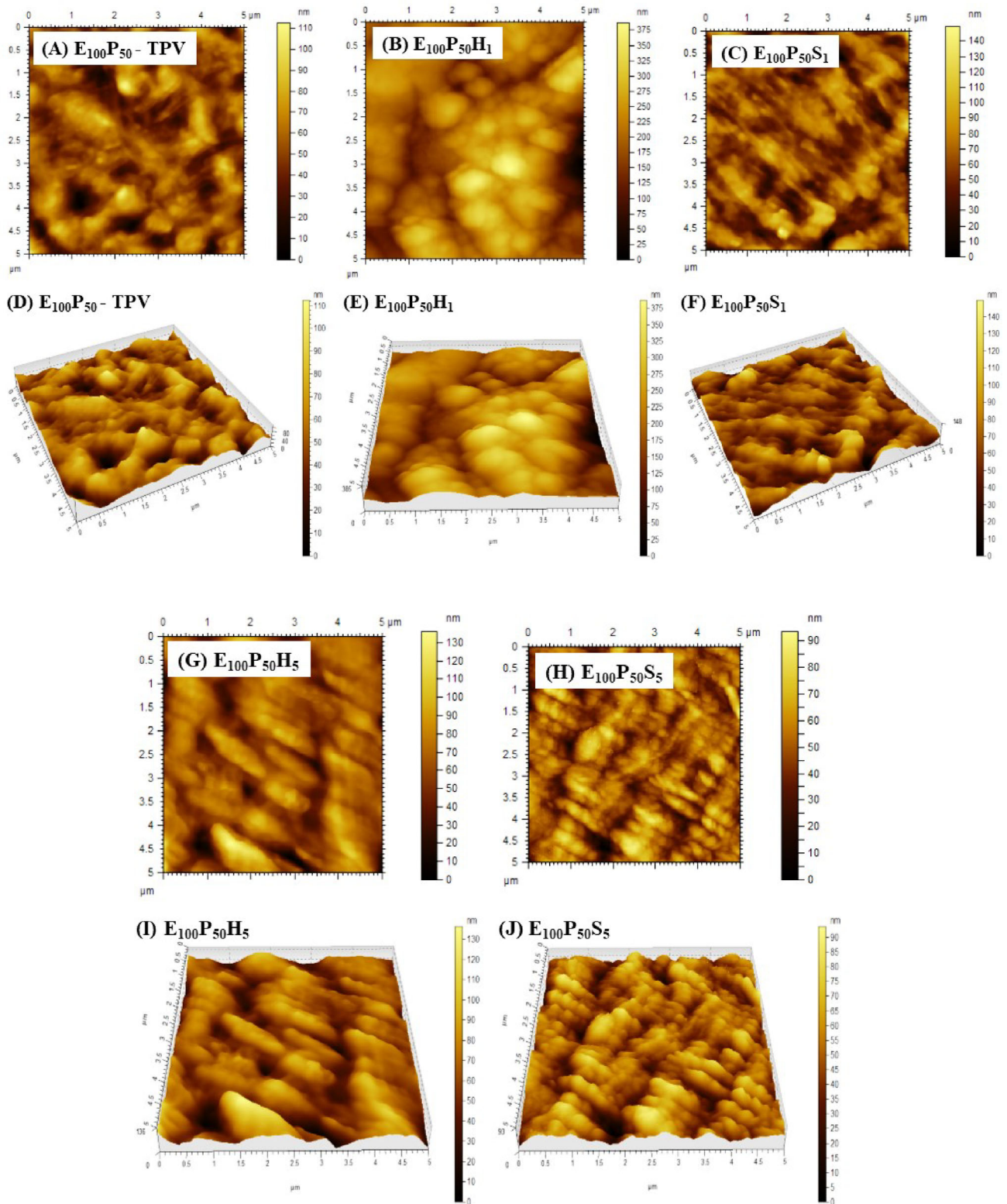


FIGURE 7 AFM topography images (A, B, C, G, H) and height images (D, E, F, I, J) of $E_{100}P_{50}$, $E_{100}P_{50}H_1$, $E_{100}P_{50}S_1$, $E_{100}P_{50}H_5$, and $E_{100}P_{50}S_5$ [Color figure can be viewed at wileyonlinelibrary.com]

images, and 3D images of $E_{100}P_{50}$, $E_{100}P_{50}H_1$, $E_{100}P_{50}S_1$, $E_{100}P_{50}H_5$, and $E_{100}P_{50}S_5$ blends are shown in Figure 7. In the current study, we have assigned brighter regions to the soft material and darker regions to harder material.^[7,9]

Figure 7A,D shows the topography image and 3D image of $E_{100}P_{50}$ blend. The existence of a two-phase morphology is evidenced from the image, which correlates the SEM images of the same sample. The

corresponding phase image shows the distribution of the hard and soft domains and also indicates micro-phase separation of the hard and soft segments. From Figure 7B,C,E-J depicts the nano-clay TPVNs and nano-silica TPVNs, respectively, at different phr of nano-fillers. We can see the uniform distribution of the nano-fillers in the PP/EPDM matrix at 1 phr filler.

Similar type of morphology has been observed from the AFM as we have seen in the FESEM study. For the pristine sample ($E_{100}P_{50}$), almost one-third area covered with the brown dark phase, which is the evident that these domains belong to the PP phase. For TPVNs, PP phase is distributed in similar fashion as observed in FESEM for $E_{100}P_{50}S_1$ and $E_{100}P_{50}H_1$. For higher filler loading of nano-clay, same morphology we can see elongated type of morphology ($E_{100}P_{50}H_5$) Figure 7G,I and for nano-silica equiposited domain type structure ($E_{100}P_{50}S_5$) had observed in Figure 7H,J.^[27,33]

4 | CONCLUSIONS

In the present work, UHMW EPDM/PP TPV and TPVNs with nano-clay and nano-silica has been developed with a fixed EPDM/PP ratio and with different nano-filler concentrations. We have studied mechanical properties of the TPVs and TPVNs, thoroughly and we can see that there is an improvement of modulus (300%) of 10% at low phr and 25% at high phr after addition of nano-clay and nano-silica in the TPV matrix. Due to incorporation of nano fillers, the crosslink density of the TPVNs are reduced as compared to the pristine TPV and the highest degree of crosslinked structure is $E_{100}P_{50}S_7$. It is also observed that at low phr of the both nano fillers degree of crosslink is least than pristine TPV and other TPVNs. Reprocessability study of the TPV and TPVNs also indicating the satisfactory results and shows ideal behavior of TPVs. The mechanical properties after second and third cycle retained up to 90%. In morphology study (AFM, SEM) suggest that after dynamic vulcanization and addition of the nano-fillers in the TPV matrix, nano-clay TPVs are forming elongated type morphology, whereas nano-silica added TPVs are showing droplet or domain type morphology at submicron level. SAXS study also proves that scattering intensity is highest for $E_{100}P_{50}S_7$ and lowest for $E_{100}P_{50}H_7$, which proves the better dispersion of the nano-silica than nano-clay in the PP/EPDM matrix. Finally, it can be concluded that nano-silica added TPVs are turned out superior, especially $E_{100}P_{50}S_7$ and $E_{100}P_{50}S_5$ than nano-clay added TPVs in terms of mechanical properties, crosslink density, and morphology point of view. We can say that the UHMW EPDM/PP TPVNs can be used as potential candidates for

application in automotive sector, such as car side panel, window seal, roof trim, cooling air guide, air bag cover, and dashboard.

ACKNOWLEDGMENT

The authors would like to acknowledge ARLANXEO, The Netherlands, for providing the EPDM rubber. We are also thankful to Anton Paar for pursuing the SAXS testing. We also thank Sanjay Pal, Anagha M. G., Mithun Das, and Rajesh De for their support.

ORCID

Kinsuk Naskar  <https://orcid.org/0000-0002-8536-4983>

REFERENCES

- [1] A. M. Gessler; W. H. Haslett, United States Patent Office, US3037954A, **1962**.
- [2] K. Naskar, J. W. M. Noordermeer, *Rubber Chem. Technol.* **2011**, 77, 955.
- [3] A. Y. Coran, R. P. Patel, *Rubber Chem. Technol.* **1978**, 53, 141–150.
- [4] A. Y. Coran, R. P. Patel, *Rubber Chem. Technol.* **1980**, 53, 781–794.
- [5] R. Rajesh Babu, K. Naskar, *Adv. Polym. Sci.* **2010**, 239, 219–247.
- [6] A. M. Gopalan, K. Naskar, *Polym. Adv. Technol.* **2019**, 30, 608.
- [7] T. Chatterjee, S. Wiessner, K. Naskar, G. Heinrich, *Express Polym. Lett.* **2014**, 8, 220.
- [8] R. Rajeshbabu, U. Gohs, K. Naskar, V. Thakur, U. Wagenknecht, G. Heinrich, *Radiat. Phys. Chem.* **2011**, 80, 1398.
- [9] T. Chatterjee, D. Basu, A. Das, S. Wiessner, K. Naskar, G. Heinrich, *Eur. Polym. J.* **2016**, 78, 235.
- [10] T. Chatterjee, N. Vennemann, K. Naskar, *J. Appl. Polym. Sci.* **2018**, 135, 1.
- [11] N. Ning, S. Li, H. Wu, H. Tian, P. Yao, G. H. HU, M. Tian, L. Zhang, *Prog. Polym. Sci.* **2018**, 79, 61.
- [12] S. Abdou-Sabet, R. P. Patel, *Rubber Chem. Technol.* **1991**, 64, 769–779.
- [13] K. Naskar, D. Kokot, J. W. M. Noordermeer, *Polym. Degrad. Stab.* **2004**, 85, 831.
- [14] M. Van Duin, A. V. MacHado, *Polym. Degrad. Stab.* **2005**, 90, 340.
- [15] M. Maiti, J. Patel, K. Naskar, A. K. Bhowmick, *J. Appl. Polym. Sci.* **2006**, 102, 5463.
- [16] K. Chatterjee, K. Naskar, *Express Polym. Lett.* **2007**, 1, 527.
- [17] W. H. Awad, G. Beyer, D. Benderly, W. L. Ijdo, P. Songtipya, M. d. M. Jimenez-Gasco, E. Manias, C. A. Wilkie, *Polymer* **2009**, 50, 1857.
- [18] B. Bhuyan, S. K. Srivastava, J. Pionteck, *Polym. Plast. Technol. Eng.* **2018**, 58, 1.
- [19] A. B. Bhattacharya, T. Chatterjee, K. Naskar, *J. Appl. Polym. Sci.* **2020**, 2, 1.
- [20] S. Doagou-Rad, A. Islam, T. D. Merca, *Polym. Compos.* **2019**, 41, 1153.
- [21] A. P. Meera, S. Said, Y. Grohens, S. Thomas, *J. Phys. Chem.* **2009**, 113, 17997.
- [22] T. Chatterjee, S. Wiessner, K. Naskar, G. Heinrich, *Polym. Eng. Sci.* **2017**, 57, 1073.

- [23] K. Naskar, J. W. M. Noordermeer, *Rubber Chem. Technol.* **2011**, 76, 1001.
- [24] S. Datta, K. Naskar, J. Jelenic, J. W. M. Noordermeer, *J. Appl. Polym. Sci.* **2005**, 98, 1393.
- [25] K. Naskar, J. W. M. Noordermeer, *J. Appl. Polym. Sci.* **2006**, 100, 3877.
- [26] P. J. Flory, J. Rehner, *J. Chem. Phys.* **1943**, 11, 512.
- [27] Z. Yang, H. Peng, W. Wang, T. Liu, *J. Appl. Polym. Sci.* **2010**, 116, 2658.
- [28] M. C. Boyce, O. Yeh, S. Socrate, K. Kear, K. Shaw, *J. Mech. Phys. Solids* **2001**, 49, 1343.
- [29] G. Beaucage, D. W. Schaefer, *J. Non-Cryst. Solids* **1994**, 172, 797.
- [30] P. K. Chattopadhyay, N. C. Das, S. Chattopadhyay, *Compos. Part A* **2011**, 42, 1049.
- [31] R. R. Babu, N. K. Singha, K. Naskar, *Express Polym. Lett.* **2008**, 2, 226.
- [32] S. Varghese, R. Alex, B. Kuriakose, *J. Appl. Polym. Sci.* **2004**, 92, 2063.
- [33] T. Chatterjee, S. Hait, A. B. Bhattacharya, A. Das, S. Wiessner, K. Naskar, *Polym. Technol. Mater.* **2020**, 59, 141.
- [34] R. R. Babu, N. K. Singha, K. Naskar, *Express Polym. Lett.* **2010**, 4, 197.

How to cite this article: Bhattacharya AB, Raju AT, Chatterjee T, Naskar K. Development and characterizations of ultra-high molecular weight EPDM/PP based TPV nanocomposites for automotive applications. *Polymer Composites*. 2020; 41:4950–4962. <https://doi.org/10.1002/pc.25765>